Contract # F49620-99-C-0024
Item # 0002AA

LIGHTWAVE® ELECTRONICS

Phase I SBIR Final Report

Project Title: **High-Power Mid-Infrared Laser Source**

Contractor: Lightwave Electronics
2400 Charleston Rd
Mountain View CA 94043

Principal Investigator: Dr. Lawrence E. Myers

Sponsor: United States Air Force
Air Force Materiel Command
Air Force Office of Scientific Research
810 North Randolph Street, Room 732
Arlington , VA 22203-1977

Technical Monitor: Maj. Daniel Johnstone, AFOSR/NE

REPORT DOCUMENTATION PAGE

AFRL-SR-BL-TR-00-

0176

1. AGENCY USE ONLY *(Leave blank)*	2. REPORT DATE	3. REPORT TYPE AND DATES COVERED
		Final 01 May 99 to 31 Oct 99

4. TITLE AND SUBTITLE
(SBIR Phase 1) High-power Mid-Infrared laser source

5. FUNDING NUMBERS
62173C
1660.01

6. AUTHOR(S)
Dr Myers

7. PERFORMING ORGANIZATION NAME(S) AND ADDRESS(ES)
Lightwave Electronics Corp
2400 Charleston Rd
Mountain View CA 94043

8. PERFORMING ORGANIZATION REPORT NUMBER

9. SPONSORING/MONITORING AGENCY NAME(S) AND ADDRESS(ES)
AFOSR/NE
801 N Randolph Street Rm 732
Arlington, VA 22203-1977

10. SPONSORING/MONITORING AGENCY REPORT NUMBER
F49620-99-C-0024

11. SUPPLEMENTARY NOTES

12a. DISTRIBUTION AVAILABILITY STATEMENT
APPROVAL FOR PUBLIC RELEASE, DISTRIBUTION UNLIMITED

12b. DISTRIBUTION CODE

13. ABSTRACT *(Maximum 200 words)*

Characterization of a practical cw mode-locked pump laser based on passive mode-locking technology.
Demonstration of a synchronously pumped optical parametric oscillator by a cw mode-locked laser with both linear and ring cavities.
Demonstration of 0.36 W threshold, pump depletion of 83%, and maximum idler power of 0.85 W at 3.6 um (with 6.9 of pump input).
Demonstration of efficient OPO operation with PPLN crystals as short a 1 cm which is one absorption length at 5 um.

14. SUBJECT TERMS	15. NUMBER OF PAGES
	16. PRICE CODE

17. SECURITY CLASSIFICATION OF REPORT	18. SECURITY CLASSIFICATION OF THIS PAGE	19. SECURITY CLASSIFICATION OF ABSTRACT	20. LIMITATION OF ABSTRACT
UNCLASSIFIED	UNCLASSIFIED	UNCLASSIFIED	UL

Standard Form 298 (Rev. 2-89) (EG)
Prescribed by ANSI Std. 239.18
Designed using Perform Pro, WHS/DIOR, Oct 94

Table of Contents

List of Figures

List of Tables

Preface

This report is the final report for the Phase 1 Small Business Innovation Research (SBIR) contract entitled "High-Power Mid-Infrared Laser Source" performed by Lightwave Electronics Corporation during the period 1 May 99 - 31 Oct 99. The principal investigator for this work was Dr. Lawrence Myers of Lightwave Electronics.

We wish to acknowledge Jim Kayser of Lightwave Electronics for building the passively mode-locked laser (Model 631) used as the pump source for this work, and Donna Howland, also of Lightwave Electronics, for performing the OPO building and testing on this program. We also appreciate Maj. Dan Johnstone of the Air Force Office of Scientific Research (AFOSR/NE) for serving as the technical monitor of the program.

1.0 Introduction

1.1 Background

The opportunity addressed by this Small Business Innovation Research (SBIR) program is to take advantage of recent developments in passively mode-locked solid-state lasers and efficient nonlinear materials for frequency conversion to develop a high-power mid-infrared (IR) source. High-power mid-IR sources are needed for IR countermeasures (IRCM), as well as commercial sector applications in remote sensing, spectroscopy, and medical instruments. While recent advances have been made in solid-state and diode lasers, it is still a challenge to meet the performance specifications and packaging requirements for the laser transmitter module for such an IRCM system. While there is work underway on direct diode laser sources, there are many challenges in developing new laser technology such as this. Thus frequency conversion of existing lasers continues to play an important role in providing mid-IR sources. In particular, devices based on frequency down-conversion of 1 μm lasers are particularly useful because they build on the existing well-established base of diode-pumped solid-state laser technology. When possible to do so, the use of components from the commercial technology base greatly lowers the cost and improves the maintainability of military systems compared to reliance on military-specific technology.

While the entire 3-5 μm atmospheric transmission band needs to be covered (as well as the 2 μm band), the longer wavelength region 4.5-5 μm has proven to be the most difficult since nonlinear materials do not operate well in this region. For example, a common system is to use the nonlinear material KTP to convert 1 μm solid-state lasers like Nd:YAG by down-conversion in an optical parametric oscillator (OPO) to the mid-IR. However KTP starts to experience high losses in the spectral range >3 μm as shown in Fig 1. The newer materials KTA and RTA are homologues of KTP with better transmission in the IR so they are preferred for use in this spectral range. Still residual absorption near the IR band edge makes their use in the range 4.5-5 μm problematic.

Thus there has been significant effort to develop nonlinear materials for the mid-IR. The materials AgS and AgSe have transmission in the 3-5 μm range but have poor thermal properties so that high-power operation is prohibited. The material ZGP has far better thermal conductivity, and its development into a high-quality, low-loss crystal has been one of the major success stories of the USAF materials development efforts. [1, 2] Multi-watt OPOs in the 3-5 μm range have been demonstrated with this material, making it one of the leading contenders for use in IRCM systems. [3] Unfortunately the residual absorption at 1 μm means that the device must be pumped at 2 μm using less common Tm,Ho-based lasers. While great advances have been made in R&D on 2 μm lasers and there are some limited medical and sensing applications, there is little reason to think that they will occupy a sizable place in industrial infrastructure compared to the ubiquitous 1 μm lasers, so the 2 μm pumped mid-IR sources have generally remained military-specific systems.

What is most needed is to have a nonlinear material that can operate at high power throughout the 3-5 μm range and also be pumped by 1 μm lasers. Such a system would be the most cost-effective approach since it would piggyback on commercial off-the-shelf technology. A recent development that has made some improvement in this situation has been quasi-phasematched (QPM) frequency conversion using periodically poled ferroelectric materials. The advantage of these materials is that they have very high nonlinearity compared to conventional crystals using birefringent phasematching. The main reason for this is that, when the need to use orthogonal polarization components in birefringent phasematching

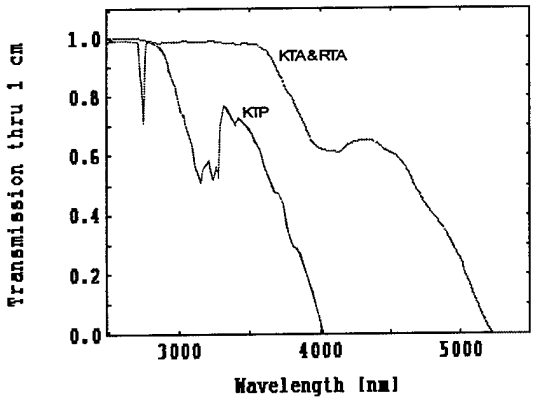

Fig 1. Normalized transmission of KTP, KTA, and RTA. [4]

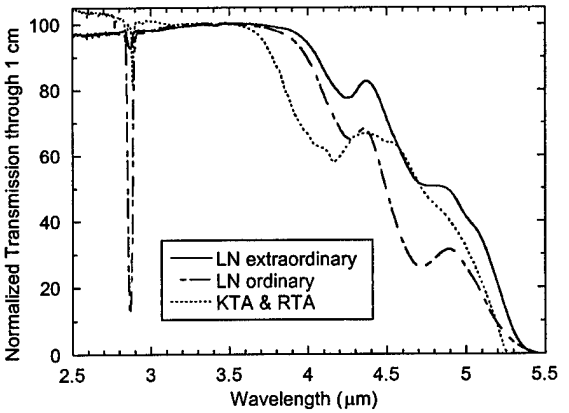

Fig 2. Normalized transmission of 1 cm thick LN and KTA/RTA. [5]

is lifted, the interaction can access the largest components of the nonlinear susceptibility which make use of all waves polarized in the same direction. Another reason is that the flexibility to engineer the phasematching properties with the design of the periodic structure allows the use of noncritical phasematching of any interaction, so that tight focusing without walk-off is possible.

The materials periodically poled lithium niobate (PPLN), KTP (PPKTP), and RTA (PPRTA) are now commercially available crystals. While they each have their pros and cons, some of the most remarkable results have been produced with PPLN, particularly in regards to generation at the longer wavelength end of the 3-5 μm range. [5] In a pulsed system pumped by 1 μm Nd:YAG Q-switched lasers, operation out to 4.9 μm has been demonstrated. [6] This is a longer wavelength than would be expected from previous use of conventional LN in the IR which required an ordinary polarized idler wave (type 1 negative birefringence) because the d_{33} QPM interaction allows the idler to be an extraordinary wave which turns out to have better transmission than the ordinary wave, as shown in Fig 2. In fact, PPLN with extraordinary polarization has better transmission in the IR than KTA or RTA which were previously considered the best materials for mid-IR generation from 1 μm lasers. Thus PPLN has become the material of choice for some applications. Lightwave has a delivered to the Navy a PPLN pulsed OPO which is now being used for IRCM tests in NATO exercises.

One of the most impressive devices enabled by PPLN has been the cw singly resonant OPO. [7] Historically it has been difficult to build cw OPOs because the threshold for single resonance is excessively high (with conventional materials) and the stability of double resonance is prohibitively sensitive. Therefore no cw OPOs have ever been developed commercially before the advent of PPLN. However the high gain, no walk-off, and noncritical phasematching of PPLN allow the cw SRO to be built simply with an off-the-shelf commercial 1 μm pump laser as shown in Fig 3. The PPLN cw SRO has produced record results in high-power cw generation with over 5 W generated at 3.5 μm and beyond. [8, 9] In addition the device is tunable as shown in Fig 4, and output as far out as 4 μm has been produced. [10]

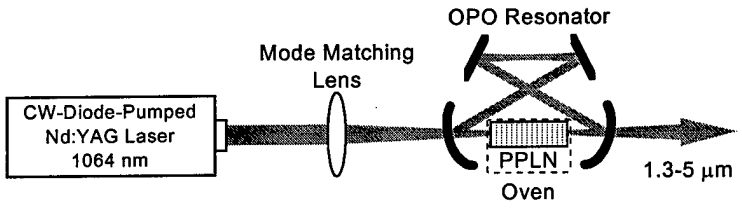

Fig 3. The cw SRO using PPLN generates multi-watt true-cw mid-IR output with off-the-shelf commercial components, but power drops off beyond 4 μm.

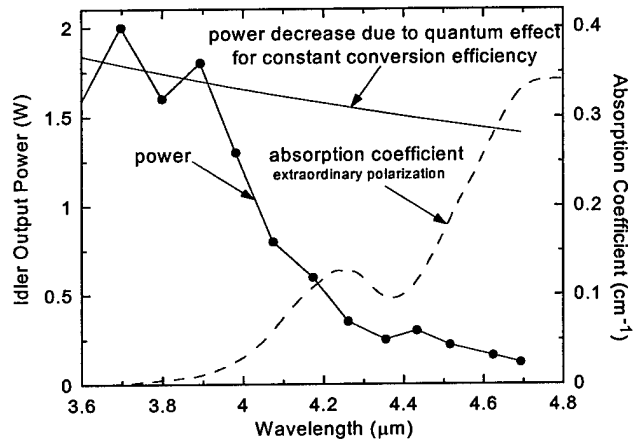

Fig 4. Tuning of PPLN cw SRO. The idler output power follows the absorption coefficient. The slanted line at the top of the graph represents the decrease in idler power that would be attributable simply to the lower quantum energy of longer wavelengths photons. The variations in the data at shorter idler wavelengths are due to the optical coatings on the crystal and resonator mirrors.

The cw SRO is an especially important accomplishment for application to IRCM systems. Most of the high-power mid-IR sources that have been produced so far have been pulsed. These sources are primarily used in IRCM systems that operate open loop, i.e. the jamming function is performed with preset modulation waveforms. However, IRCM systems that are under development to address the more sophisticated threats employ a closed-loop approach that uses feedback from interrogation of the seeker head to adjust the jam code for maximum effectiveness against the particular missile. [11] The interrogation relies on illuminating the seeker head and decoding the modulation in the retro-reflected return. For maximum robustness against unknown or variable threats, a cw laser is needed for the interrogation function. For the next generation of capable IRCM systems, the cw SRO has offered a major advance in the technology of high-power cw sources in the mid-IR. These devices have been developed into compact and efficient packages that are now being deployed in laboratory test facilities. Shown in Fig 5 is an example of a PPLN cw SRO that is in use at the Guided Weapons Test Facility at Eglin AFB.

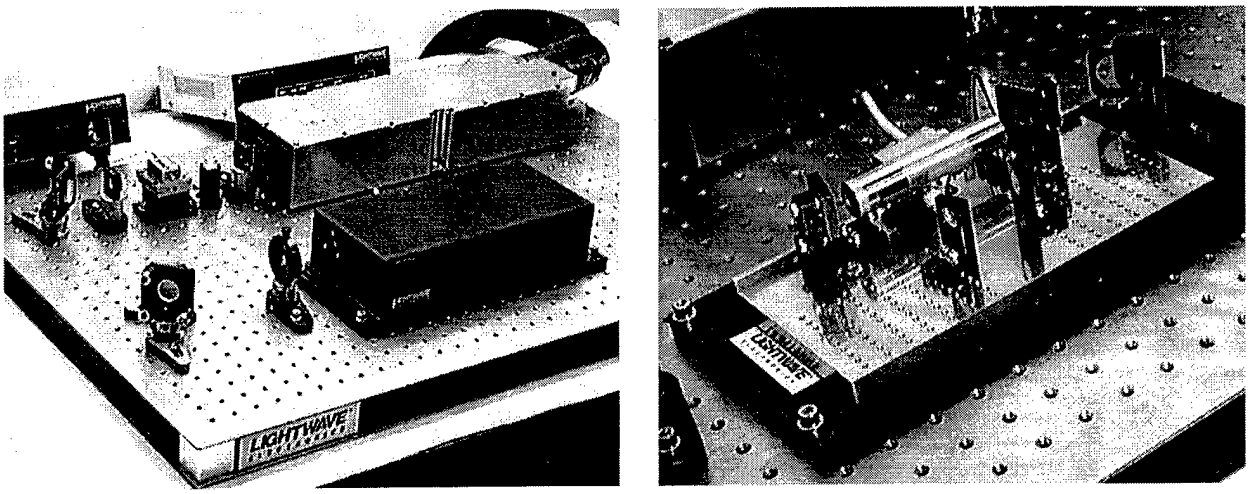

Fig 5. Example of a PPLN cw SRO delivered by Lightwave Electronics for use in IR seeker testing at Eglin AFB. It produces 1.5 W at 4 μm.

While tunable output in the 3-5 μm range can been produced with the cw SRO, as seen in Fig 4, the power drops off at the longer wavelengths due to absorption in the PPLN material. Since PPLN is strongly absorbing beyond 4.3 μm, only the idler generated in the last absorption length L_{abs} is essentially extracted from the crystal, as shown in Fig 6. Thus it is apparent that the drop-off in power observed in the cw SRO is primarily associated with the shorter crystal length that is effective in generating idler output. For increasing the idler generation, the conversion in one absorption length must be maximized. The conversion per unit length can be increased by increasing the gain with higher pump intensity, which can be obtained by using a mode-locked (ML) laser. In fact, the use of a ML pump laser has enabled operation of PPLN SROs with output wavelengths 6.3 μm which is well into the region of strong absorption. [12]

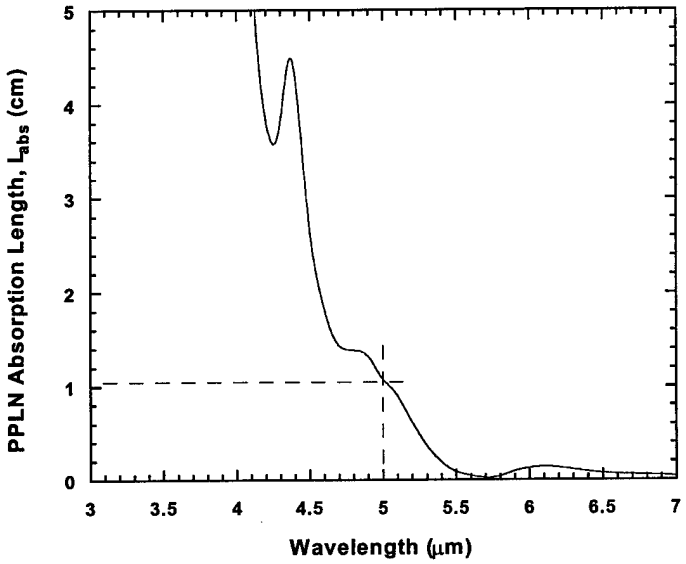

Fig 6. The idler output is effectively only that generated in the last absorption length of the crystal, i.e. $\alpha L_{abs} = 1$ for absorption coefficient α.. For 5 μm generation in PPLN, L_{abs} = 1 cm, so the conversion in that length must be maximized.

While the maximization of conversion depends on the particular experimental detail (e.g. focusing conditions), the plane-wave limit is a useful simplification for obtaining analytical insight. In the plane-wave case without depletion, ignoring absorption because we are only considering the portion of crystal $L<L_{abs}$, the parametric gain in a crystal of length L is approximated by [13]

$$gain = \frac{2\pi^2 d^2 L^2}{n_1 n_2 n_3 c \varepsilon_0 \lambda_{pump}^2} I_{pump}$$

where d = effective nonlinear coefficient, λ_{pump} = pump wavelength, I_{pump} = pump intensity, and n_1, n_2, n_3 = refractive index for the idler, signal, and pump respectively. With other parameters constant, the gain can be increased by increasing the pump intensity. In the case of a ML laser, the laser power is delivered in a train of short intense pulses. As shown in Fig 7, the peak intensity is increased relative to the average intensity by

$$\frac{I_{peak}}{I_{avg}} = \frac{T}{\tau} = \frac{1}{\tau f_{PRF}}$$

where f_{PRF} = pulse repetition frequency. In a typical cw ML 1 μm solid-state laser, τ = 10-20 ps and f_{PRF} = 100 MHz, so the peak intensity enhancement factor is ~500-1000. Thus the idler generation in the crystal length L_{abs} will be orders of magnitude higher with a ML laser compared to a straight cw laser.

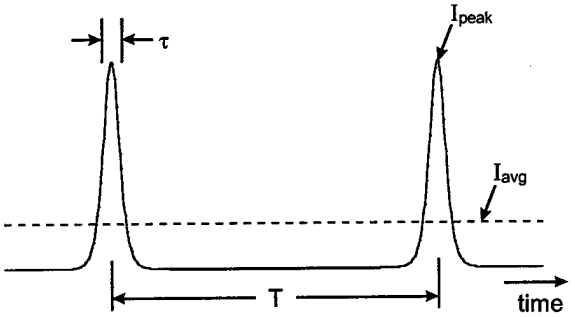

Fig 7. Enhancement of peak intensity of over average intensity in a ML laser. Typical enhancement factor for a passively ML Nd:YAG laser is $I_{peak}/I_{avg} = T/\tau$ = 500-1000.

Because the gain per unit length is substantially higher in the ML approach, it is also expected to help in regards to other problems which are encountered in high-power nonlinear optics. In particular, the ability to use shorter crystals will cut down on the effect of thermal de-phasing and thermal focusing, and will increase the acceptance bandwidths. [14] Larger acceptance bandwidth together with higher gain make the ML SRO less susceptible to loss than the true-cw device, and hence more tolerant of any remaining thermal effects. Also with the capability to use shorter crystals, the new quasi-phasematched material PPRTA can be used, which is only available in ~20 mm crystals rather than the 40-50 mm long crystals used for PPLN cw SROs. (PPKTP is not an improvement since it has substantially higher long-wavelength absorption than either PPLN or PPRTA). Other materials that are under development at this time include periodically poled versions of MgO-doped lithium niobate, lithium tantalate, and potassium niobate. Compared to the cw SRO, the ML SRO is a preferred test vehicle because it is more accommodating of the relatively short lengths and sub-optimal domain quality compared to PPLN that might be expected in newly emerging materials. The ML SRO implementation is also compatible with techniques that have been proposed to increase idler output and reduce thermal susceptibility, such as multiple outcoupling of the idler. One technique that looks particularly promising for increasing idler output is to cascade the OPO with an intracavity difference frequency mixer (DFM) to generate extra

idler photons from the signal photons. This technique has been shown to work with both pulsed and cw ML OPOs but has not yet been applied to the regime of strong idler absorption. [15, 16]

To take advantage of the high peak intensity, the OPO must be synchronized to the pump laser so that the pump pulse and the resonant signal pulse overlap in the crystal. Perfect synchronization requires matching the cavity length of the laser and OPO resonators, but fortunately the tolerance on achieving this match is looser than might be expected. [17] The criterion for synchronized pulses is based on overlapping the pulses to within some fraction of the pulse length within the lifetime of the pulse in the cavity. Since the pulse length of $\tau = 10$ ps corresponds to a pulse extent in space of 3 mm, the tolerance for synchronization is achievable by strictly passive means and good mechanical design without having to resort to active cavity-length control. There is much interest in the generation of fs pulses with passively ML lasers, and these would have proportionately higher peak intensities than the ~10 ps pulses that are typical with Nd:YAG systems. (Nd:YLF and Nd:YVO_4 give slightly shorter pulses than Nd:YAG, but they are still in the ps range.) However, working in the fs regime significantly increases the complexity of synchronization and adds the further complication of having to avoid pulse broadening caused by group velocity dispersion. While Nd:YAG and related lasers can not produce sub-ps pulses because of their limited gain bandwidth, they have the important advantage that they can be directly diode pumped, can operate at high average power, and draw on a substantial commercial development base, which can not be said for much of the fs laser technology. Fortunately fs pulses are not needed for this application since pulses ~10 ps provide ample nonlinear drive given the high nonlinearity of PPLN and other QPM materials.

A ML laser can be considered effectively a cw source in applications that are not sensitive to the modulation frequency of the high-repetition-rate pulses. This is the case in IRCM systems since pulse repetition frequencies lie outside the receiver bandwidths. While there is no receiver penalty for the ML format and there is a definite transmitter benefit in generating high-power mid-IR radiation efficiently, there is a perceived complexity disadvantage in using a ML laser in an IRCM system. However, recent advances in the development of passively ML cw-diode-pumped solid-state lasers make a ML laser of the type suitable for IRCM no more complicated than similar cw lasers. The principle technology that has made this possible is the semiconductor saturable absorber, which appears in two variants: semiconductor saturable absorbing mirrors (SESAM) and saturable Bragg reflectors (SBR). [18, 19] The differences between these two devices are either great or small depending on the emphasis and who you ask, but they both rely on distributed Bragg reflector stacks and semiconductor saturable absorbing thin films fabricated by epitaxial growth (MBE or MOCVD). For mode-locking of Nd:YAG-like lasers, both approaches have produced similar results. These lasers are essentially as simple as a cw laser with the same cavity, the only difference being that one of the end mirrors is replaced with the SESAM or SBR element. As compared to actively ML lasers, the passive approach is simpler, more compact , and more robust because its does not need the high-Q resonant AO modulator, its associated RF driver, and active cavity-length control to match the cavity resonance to the RF drive frequency. Also passive mode-locking generally produces shorter pulses than active systems. [20] The SESAM/SBR approach is simpler that other passive mode-locking schemes, such as additive pulse mode-locking and Kerr Lens mode-locking. [20] Additive pulse mode-locking is achieved by nonlinear modulation of a coupled external resonant cavity, which require interferometric stabilization of the lengths of the two cavities. This is not an approach which lends itself to robust implementation, so it is primarily restricted to laboratory research systems. In Kerr lens mode-locking, a phase shift induced by nonlinearity in the

laser medium decreases the resonator mode size which is coupled to cavity loss by an intracavity aperture. While the Kerr lens technique is simple in principle, it requires a sensitive cavity design to produce the required mode size changes, which is typically not desired for a robust, reliable product. Also the mode-locking is not self-starting so an additional starting mechanism is often required (such as cavity mirror perturbation or a SESAM/SBR).

In addition to the passive mode-locker itself, the laser gain module is critical to the success of a practical, robust ML laser. Lightwave has developed a gain module using our patented Direct Coupled Pump (*DCP*™) technology which is a workhorse laser engine that has been well received by the commercial laser marketplace. In a *DCP*™ engine, high-power cw diode laser bars directly pump the laser rod without any intervening beam-shaping optics. This approach is manufacturable, economical, and reliable in the field. It is the base of a Lightwave commercial product line, with over 1,500 lasers now in use worldwide. *DCP*™ lasers are known for their high efficiency (typ 30%) and good beam quality (typ $M^2<1.1$). Currently the cw version of our *DCP*™ laser operates at 15 W with a 25 W version under development. This laser has been shown to be excellent for pumping the cw SRO to generate high-power mid-IR, and for high-power mode-locking using SESAM/SBRs. [10, 21]

With the efficient and practical pump laser technology afforded by *DCP*™ and SESAM/SBRs, major advances will be possible in nonlinear frequency conversion. The prospect of generating significant power levels out to 5 μm is of high national importance for IRCM, as well as potentially benefiting medical and sensing applications. In addition, robust high-power passively ML solid-state lasers are expected to play a significant role in other applications requiring efficient frequency conversion to visible and UV wavelengths including machining, rapid prototyping, and laser-based displays. A high-power RGB display system has already been demonstrated in Germany using amplified low-power ML lasers and conventional nonlinear materials. [22] The combination of techniques to be developed under this program will significantly further such applications along the road to commercialization.

1.2 Program Objectives

The scope of the overall research program is to develop high-power sources based on frequency conversion of passively ML diode-pumped solid-state lasers. The technical objective is to develop a high-power cw-like source in the mid-IR with emphasis on the range 4.5-5 μm, based on a passively ML 1 μm laser. Our goals for the Phase 1 portion of the program are:

1. Demonstrate a robust, high-power cw ML laser based on a manufacturable passive mode-locking approach.
2. Demonstrate improved mid-IR generation with a synchronously pumped OPO.

2.0 Passively Mode-locked Pump Laser

Lightwave Electronics has been developing a high-power cw ML laser based on our Direct-Coupled Pump (*DCP*™) diode-pumped Nd:YAG gain module technology. This is a laser gain module that forms the core of our commercial product line of high-power cw and Q-switched Nd:YAG lasers. In a Phase 2 SBIR program supported by NIH, we have extended this technology to cw mode-locked format. The key to this extension is the development of a passive mode-locking element based on a semiconductor saturable absorber. We have demonstrated that this element works well with our laser engine, is resistant to Q-switching instability with our cavity designs, and does not damage even up to the 12 W level of cw mode-locked operation. We have developed this technology to the point of introducing a commercial product based on it, which we designate the Model 631.

A schematic of the ML pump laser is shown in Fig 8. The laser uses the *DCP*™ diode-pumped gain module and is mode-locked by inserting a SBR in place of a standard dielectric-coated end-mirror and adjusting the amount of output coupling. The standard design for an SBR involves embedding a quantum-well saturable absorber layer into a Bragg reflector stack. Two key parameters in the SBR design are the saturation fluence and the modulation depth, which can be adjusting by changing the number and placement of the quantum wells. This Phase 1 program has further contributed to the development of the Model 631 laser. We completed a detailed characterization of the first prototype laser. As shown in Fig 9, this laser had a pulse length of 35 ps with a sech^2 temporal profile, corresponding to 1.6 times the transform limit of the measured optical spectrum. The beam spatial profile was TEM_{00} with beam quality factor $M^2 = 1.10$ and circularity of 0.88 (i.e. ratio of minor to major axes). The pulse repetition rate of this laser was 127 MHz and the pulse train shows no timing jitter on qualitative inspection.

The significance of this accomplishment is that we have developed a simple mode-locked laser which is self-starting with turnkey operation. This laser has robustness and performance comparable to our other commercial products in the *DCP*™ family, making it compatible with the needs of industrial and military applications. It will make an excellent pump source for efficient nonlinear frequency conversion, since it offers a cw-like output format (repetition rates >10 MHz are effectively cw for many applications) but with peak power 225 times higher than that of a cw laser with the same average power, i.e. 1.8 kW peak power vs. 8 W average power. This laser was used as a pump source for the OPO experiments described in the following section.

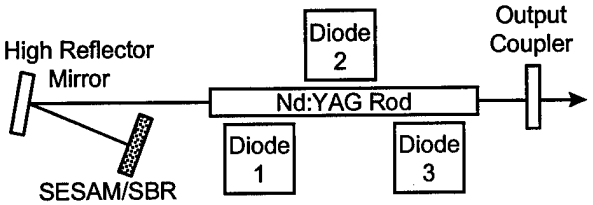

Fig 8. Schematic of the Model 631 pump laser cavity. The passive mode-locking is achieved by using a SBR in place of a conventional end-mirror. As opposed to active mode-locking, no cavity-length control is required. The laser used on this program produced 35 ps pulse at 127 MHz with 8 W output power.

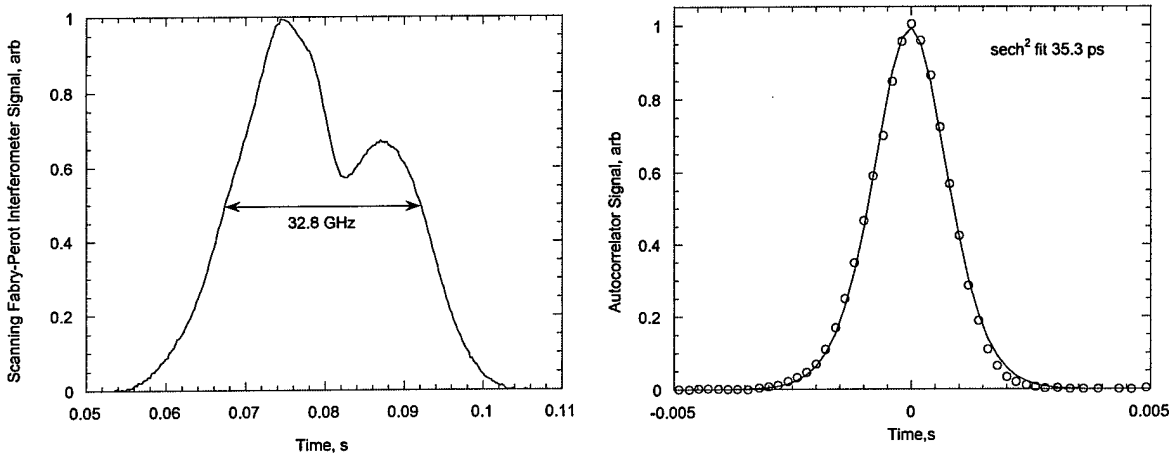

Fig 9. Temporal and spectral characterization of the Model 631 laser. a) Scanning Fabry-Perot interferometer trace of optical spectrum. b) Autocorrelation trace of mode-locked pulse. The data fits a $sech^2$ temporal profile with 35 ps full width at half maximum (conversion factor 20.4 ps/ms), which is 1.6 times the transform limit of the measured optical spectrum.

3.0 Synchronously Pumped OPO

Based on the specs of the laser described in Section 2.0, we designed the synchronously pumped OPO. Compared to the cw and Q-switched pumped PPLN OPOs that we have worked with previously, this OPO has a further design constraint, which is that the round-trip time of the resonant signal pulse must be synchronized with the arrival time of pulses from the pump laser. [5, 23] We adapted our OPO modeling programs which predict threshold, cavity mode, and pump mode-matching, to include the synchronization constraint.

For the 127 MHz pump laser, the OPO round-trip cavity length will be 2.4 m for lowest-order synchronization. This makes for a long OPO cavity, but it is no longer than the laser cavity and it can be packaged in more compact form by using folding mirrors and multi-pass paths. We based the design on the use of a 50 mm long PPLN crystal, since we had experience with this length in the cw case. For our first design, we used a linear cavity because it is easier to achieve synchronization. The reason for this is that the end mirrors of the cavity are at normal incidence which allows the cavity length to be adjusted without affecting the resonator alignment. In the case of a ring cavity, if we use a standard four-mirror bow-tie configuration, the cavity length and resonator alignment are coupled through the mirror adjustment. An advantage of a ring is that the losses are lowered because the crystal surfaces and mirrors are encountered only once for every round trip, while in the linear cavity, the crystal surface and the interior mirrors are encountered twice per round trip. The alignment and cavity length in the ring cavity can be decoupled with use of a delay leg at the expense of additional complexity and intracavity elements. In our case, the high nonlinearity of PPLN and the high peak power of the mode-locked pump laser should put us many times above threshold with our available pump power of ~8 W. Therefore the simplicity of the linear cavity outweighs its loss penalty in our initial setup. We selected 150 cm radius

of curvature for the two mirrors which form the mode in the PPLN crystal, and we designed the conditions for mode-matching the pump laser to the resonator mode.

The layout of the OPO set up is shown in Fig 10. The PPLN crystal was 50 mm long and 0.5 mm thick with 29.0 μm grating period. The mirrors with 150 cm radius of curvature gave a 39 μm radius signal mode at ~1.5 μm wavelength. For perfect mode-matching, the pump beam should be 33 μm radius, but the actual pump beam was focused into the crystal with 52 μm radius waist. The mirrors had coatings that were highly reflecting at the signal wavelength and >90% transmitting at the pump and idler wavelengths (~3.6 μm). The PPLN crystal was operated at 150 °C to avoid photorefraction, as is typical for PPLN, and it had antireflection coatings that were optimized for lowest loss at the signal and >90% transmission at the pump and idler. The low round-trip feedback of the idler (<<1%) ensured singly resonant operation at the signal only.

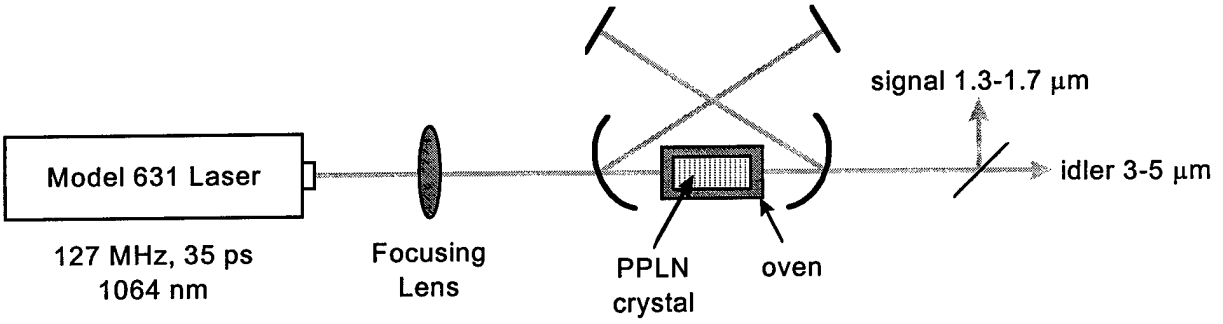

Fig 10. Layout of synchronously pumped ML OPO with linear cavity.

We set the initial cavity length by physically measuring the positions of all cavity mirrors. Next we aligned the cavity, then adjusted the cavity length until we achieved synchronism with the pump laser and the OPO started operating. We found that the cavity length was relatively insensitive to the mirror positions which means that stabilization in a product can be readily achieved with our standard commercial packaging without the need for active cavity-length control. The full width at half-maximum power due to length detuning was 2.4 mm round-trip, which is ~27% of the 30 ps laser pulse. As shown in Fig 11, we measured a threshold of 1.3 W and a maximum pump depletion of 70% at 5.9 times above threshold. We measured a maximum idler power of 1.1 W with 7.7 W of pump, which is 77% of the quantum limit given by the pump depletion. Idler power closer to the theoretical limit can be obtained by reducing losses in the output optics. The OPO ran very strongly, but the threshold was higher than the calculated value of 51 mW, which could be accounted for by several factors that are discussed further in Sections 4.0 and 5.2. In addition, we did not spend as much time optimizing the linear cavity as the ring cavity which we built next.

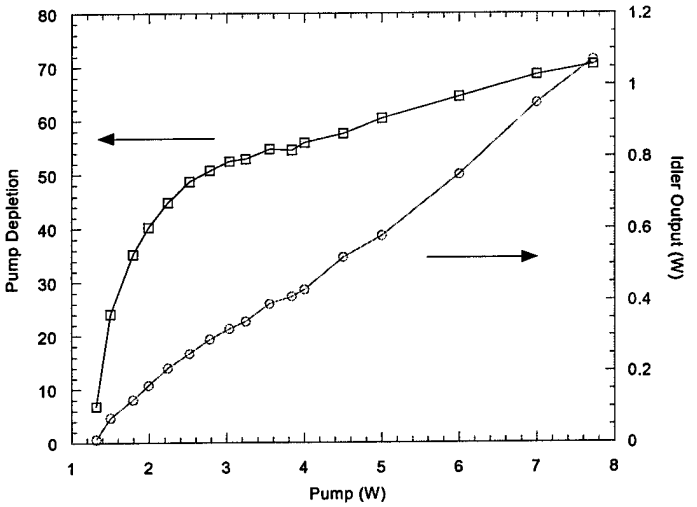

Fig 11. Pump depletion and output idler power at 3.6 μm vs. input pump power for linear cavity.

We built a ring cavity using a four-mirror bow-tie configuration as shown in Fig 12. We were concerned that synchronization would be harder to achieve because the cavity length and resonator alignment are coupled through the mirror adjustment. However, we found that the OPO was surprisingly easy to build, using a similar technique as for the linear cavity. We positioned the mirrors first based on a physical measurement, then we aligned the cavity. Next we adjusted the cavity length incrementally, realigning the mirrors as we did so, until synchronism was achieved and the OPO oscillated. This procedure was easier than we had thought it might be, and the cavity length was far less sensitive to length detuning than we had anticipated, even without the introduction of a delay leg to decouple the length adjustment from the alignment. Thus even in the case of the ring synch-pumped OPO, our standard commercial packaging will provide a robust, reliable product.

The ring cavity was built with the same cavity mode as the linear cavity using the same mirrors, which resulted in the cavity round-trip length being half that of the liner cavity (since the linear cavity passes each leg twice per round trip while the ring passes each leg once). Thus the resonant pulse in the ring cavity matched up with a pump pulse on every other cavity round-trip, and the loss per pump pulse was the same as the linear cavity. If the cavity length of the ring OPO were doubled to match the laser repetition rate, then the losses per pump pulse in the ring cavity would be approximately half those of the linear cavity which would lower the threshold. We will optimize the design in this way in the future.

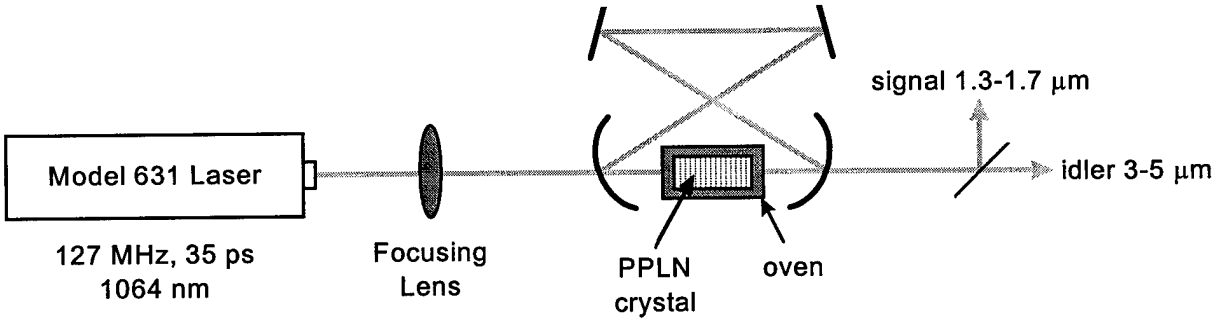

Fig 12. Layout of synchronously pumped ML OPO with ring cavity.

In this experiment, the cavity mode had a waist of 55 μm at the signal, which corresponds to a mode-matched pump waist of 46 μm. The actual pump waist was 52 μm. The focusing of the signal was such that the crystal length was 1.85 times the confocal parameter, so that the near-field analysis used in the threshold calculation was more applicable. As shown in Fig 13, the measured threshold power was 360 mW compared to a calculation of 0.10 W (12% round-trip loss assumed), using the expression in Section 4.0. We measured a maximum pump depletion of 83% at 19 times above threshold. We measured a maximum idler power of 0.85 W with 6.9 W of pump, which is 50% of the quantum limit given by the pump depletion. The full-width at half-maximum power due to length detuning was 1.7 mm round-trip, which is ~19% of the 30 ps laser pulse.

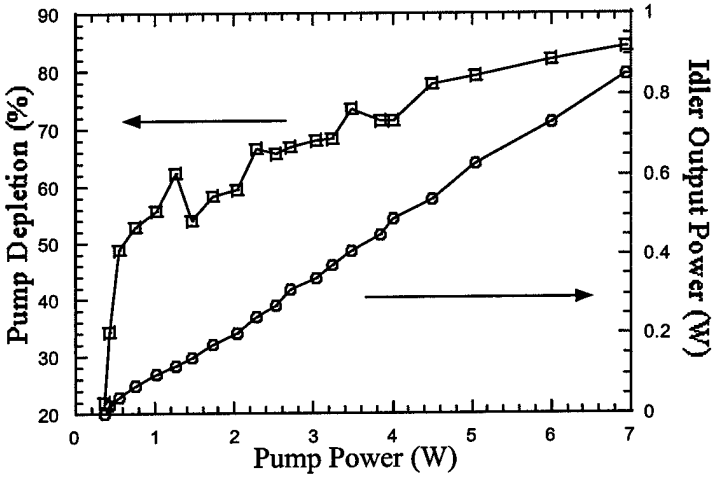

Fig 13. Pump depletion and output idler power at 3.6 μm vs. input pump power for ring cavity.

4.0 Crystal Length Scaling

The strategy for extending the operating wavelength of the mid-IR OPO depends on being able to operate with shorter crystals. In fact, the desired crystal length is less than the absorption length of the crystal (1 cm at 5 μm) as discussed in Section 1.0 (see Fig 6). We began our experiments with a 50 mm-long crystal because of our prior experience with cw OPOs using that length, but we also used shorter crystals to demonstrate the feasibility of our approach.

To calculate the predicted threshold, we used an expression based on parametric gain with a Gaussian beam in the near field. [24, 25] The simplified equation for the threshold average power P_{th} is

$$P_{th} := \frac{\alpha}{L^2} \cdot \frac{n_s \cdot n_i \cdot n_p \cdot \varepsilon_0 \cdot c^3}{2 \cdot \omega_s \cdot \omega_i \cdot d_{eff}^2} \cdot \frac{\pi \cdot w_p^2}{g_s \cdot g_t}$$

where

n_m =-refractive index (m = signal, idler, or pump) = 2.2

c = speed of light in vacuum = 3 x 10^8 m/s

α = round-trip loss (including output coupling) = 6% assumed

w_m = average radius of the respective beam

τ_m = pulse length of the respective beam

d_{eff} = effective nonlinear coefficient = $(2/\pi)d_{33}$ = 14 pm/V

ω_m = angular frequency of the respective beam = $2\pi c/\lambda_m$

λ_s = signal wavelength ~ 1.5 μm

λ_i = idler wavelength ~ 3.6 μm

L = crystal length

F_{ML} = mode-locking enhancement factor = $1/(\tau_p \, PRF)$

$$g_s := \frac{w_p^2}{w_s^2 + w_p^2}$$

$$g_t := \sqrt{\frac{\tau_p^2}{\tau_s^2 + \tau_p^2}}$$

The factors g_s and g_t account for the spatial and temporal overlap of the pump and resonant signal assuming TEM_{00} beams and Gaussian pulses. [25] In our experiments, g_s = 0.48, 0.46, 0.44, 0.37 for 10, 15, 20, 50 mm-long crystals respectively, and g_t = 0.76 for all pulse lengths. Group velocity walk-off has been ignored because it is negligible for all pulse lengths and crystal lengths involved in our experiments.

Table 1 shows the operating parameters for the various PPLN crystals that we used. All crystals had the same grating, Λ = 29.0 μm, and the same antireflection coatings that were optimized for lowest loss at the signal and >90% transmission at the pump and idler. We used a linear cavity for the OPO and the same curved mirrors with 150-mm radius of curvature. All the crystals were operated at 150 °C again to avoid photorefraction. For each crystal length, we adjusted the mirror positions to give approximately the same size of the signal mode in the resonator. Note that improvements were made to the laser during the course of these measurements, resulting in shortening of the pulse length from 31 ps to 23ps.

The measured threshold is significantly higher than the calculated threshold in all cases. This discrepancy may be due to higher round-trip losses than we estimated (6% assumed). Also the theory is based on a Gaussian beam near-field analysis while the focusing conditions of this experiment fail to obey this condition to varying degrees. Note that shorter crystals with looser focusing closer to meeting the near-field condition give better agreement with the theory. The spectral acceptances of the OPO crystals are negligible in all cases since they are much larger than the laser spectrum of 33 GHz shown in Fig 9.

Table 1. Collection of experimental data for the variation in PPLN crystal length.

Crystal length	50 mm	20 mm	15 mm	10 mm
Focusing parameter $\xi = L/b$ [a]	4.69	0.82	0.63	0.43
Pump threshold, calculated	0.10 W	0.18 W	0.26 W	0.47 W
Pump threshold, measured	1.3 W	2.5 W	2.7 W	3.9 W
Maximum pump power / times above threshold	7.7 W / 5.9x	7.2 W / 2.9x	7.09 W / 2.6x	7.0 W / 1.8x
Maximum pump depletion [b]	70%	63%	61%	37%
Maximum idler power / % of the quantum limit [b]	1.1 W / 70%	0.65 W / 49%	0.67 W / 53%	0.35 W / 47%
Pulsewidth of laser	31 ps	25 ps	25 ps	23 ps
FWHM cavity length detuning (single-pass distance) [b]	2.4 mm	1.0 mm	0.98 mm	0.18 mm
Detuning as % of the laser pulsewidth	26%	13%	13%	3%
Pump spectral acceptance FWHM (30 GHz pump spectrum) [c]	3540 GHz	2150 GHz	1580 GHz	618 GHz

a. Crystal length L relative to the confocal parameter of the signal $b = 2\pi w_0^2/\lambda$. [26]
b. Measured at maximum pump power.
c. Calculated using standard dispersion relations of [27].

As expected, the cavity length detuning range decreases with shorter crystal length because the threshold increases while the maximum pump power is fixed. However, the threshold does not scale with the expected $(1/L^2)$ dependence on crystal length. The data more closely follows a dependence of $(1/L^{0.7})$. This is possibly due to the change in focusing conditions for the different crystal lengths as described above, while the theory is valid for strictly near-field.

5.0 Conclusions

5.1 Highlights of accomplishments

- Characterization of a practical cw mode-locked pump laser based on passive mode-locking technology.
- Demonstration of a synchronously pumped optical parametric oscillator pumped by a cw mode-locked laser with both linear and ring cavities.

- Demonstration of 0.36 W threshold, pump depletion of 83%, and maximum idler power of 0.85 W at 3.6 μm (with 6.9 W of pump input).
- Demonstration of efficient OPO operation with PPLN crystals as short a 1 cm which is one absorption length at 5 μm.

5.2 Discussion

The results of Sections 2.0 and 3.0 have shown that the passively mode-locked laser is an effective source for synchronous pumping of high-power singly resonant OPOs. While mode-locked lasers are often regarded as scientific instruments that are difficult to operate and maintain, we have shown that the new generation of passively mode-locked systems are as robust and practical as standard industrial and military lasers. We also showed that the synchronously pumped OPO has relatively tolerant cavity-length acceptance so it too can be manufactured as a reliable product. The laser and OPO approach that we have taken on this program has the potential to be a useful system for lab and field operation in a military environment.

The data on scaling of crystal length discussed in Section 4.0 is of critical importance for projecting the extension of the operation of this system into the longer mid-IR range. The key benchmark was operation of the OPO with a crystal 10 mm long, which is less than one absorption length through the entire 3-5 μm band. This result validates our approach based on a mode-locked laser and synchronously pumped OPO , since a comparable cw system could not even reach threshold with these short crystals. The high peak power of the mode-locked scheme not only enables the OPO to operate but also makes it more stable and less susceptible to thermal problems in the OPO crystal.

6.0 Recommendations

The Phase 1 program successfully achieved the critical technology demonstrations required to proceed into Phase 2. These key technologies are a practical synchronously pumped OPO based on a robust passively mode-locked solid-state laser, and the operation of the OPO with short crystals which allows scaling into the mid-IR region beyond 4.5 μm. The technology demonstrated in this program will enable a high-power mid-IR source suitable for IRCM systems and other frequency conversion applications such as material processing and projection displays.

In the follow-on Phase 2 program, the power of this system will be scaled to the ~5 W level and the wavelength range will be extended to cover the long-wavelength mid-IR band. We will use the Model 631 passively mode-locked laser with amplifiers to increase the pump power to 50 W at 1064 nm. We will pump the OPO to produce ~5 W output in the 4-5 μm band. We will use PPLN as the OPO crystal in our baseline approach since it is believed to have the best infrared transmission; however, we will also consider other materials which become viable candidates with higher pump powers where reaching oscillation threshold is not an issue. We will choose the best material that maximizes the conversion to the long idler wavelengths without inducing excessive thermal problems. We will also investigate alternative architectures such as cascaded difference frequency mixing to increase idler output and an OPO operating ~2 μm with intracavity difference frequency generation which minimizes

the effect of idler absorption on the OPO. [15, 16, 28] We will package the system and deliver it to a government laboratory for use in IRCM field tests. The deployment of this high-power cw mid-IR source will significantly advance the state of the art in IRCM systems for closed-loop jamming.

7.0 References

1. F. K. Hopkins, N. C. Fernelius, M. C. Ohmer, D. E. Zelmon, and U. B. Ramabadran, "Nonlinear optical crytasl development at the USAF Wright Laboratory," in *National Aerospace and Electronics Conference* (1995).
2. P. G. Schunemann, P. A. Budni, L. Pomeranz, M. G. Kinghts, T. M. Pollack, and E. P. Chicklis, "Improved $ZnGeP_2$ for high-power OPOs," in *Advanced Solid State Lasers*, OSA Trends in Optics and Photonics 10 (Optical Society of America, Washington, DC), p. 253 (1997).
3. L. Pomeranz, P. A. Budni, P. G. Schunemann, T. M. Pollack, P. A. Ketteridge, I. Lee, and E. P. Chicklis, "Efficient power scaling in the mid-IR with a $ZnGeP_2$ OPO," in *Advanced Solid State Lasers*, OSA Trends in Optics and Photonics 10 (Optical Society of America), p. 259 (1997).
4. SNLO nonlinear optics code available from A. V. Smith, Sandia National Laboratories, Albuquerque, NM 87185-1423.
5. L. E. Myers and W. R. Bosenberg, "Periodically poled lithium niobate and quasi-phasematched optical parametric oscillators," IEEE J. Quantum Electron. **33**, 1663-1672 (1997).
6. L. E. Myers, R. C. Eckardt, M. M. Fejer, R. L. Byer, and W. R. Bosenberg, "Multigrating quasi-phase-matched optical parametric oscillator in periodically poled $LiNbO_3$," Opt. Lett. **21**, 591-593 (1996).
7. W. R. Bosenberg, A. Drobshoff, J. I. Alexander, L. E. Myers, and R. L. Byer, "Continuous-wave singly resonant optical parametric oscillator based on periodically-poled $LiNbO_3$," Opt. Lett. **21**, 713-715 (1996).
8. S. C. Tidwell, J. Seamans, and P. Roper, "Moderate-power cw pumped PPLN," in *Conference on Lasers and Electro-Optics*, 1997 OSA Technical Digest Series 11 (Optical Society of America, Washington, D.C.), paper CPD25 (1997).
9. J. I. Alexander, L. E. Myers, and R. Wallace, "7.3 W output power at 3.52 μm from a singly resonant cw PPLN OPO," in *Center for Nonlinear Optical Materials Annual Review*, (CNOM, Stanford University) (1999).
10. W. R. Bosenberg, A. Drobshoff, J. I. Alexander, L. E. Myers, and R. L. Byer, "93% pump depletion, 3.5-W continuous-wave, singly resonant optical parametric oscillator," Opt. Lett. **21**, 1336-1338 (1996).
11. C. J. Tranchita, K. Jakstas, R. G. Palazzo, and J. C. O'Connell, "Active infrared countermeasures," in *Countermesaure Systems*, D. H. Pollock, ed., (Infrared Information Analysis Center, Environmental Research Institute of Michigan, Ann Arbor, 1993).
12. L. Lefort, K. Puech, and D. C. Hanna, "Optical parametric oscillation out to 6.3 mm in peridiodically poled lithium niobate under strong idler absorption," Appl. Phys. Lett. **73**, 1610 (1998).

13. R. L. Byer, "Optical parametric oscillators," in *Quantum Electronics: A Treatise*, H. Rabin and C. L. Tang, ed. (Academic, New York, 1975), pp. 587-702.

14. M. M. Fejer, G. A. Magel, D. H. Jundt, and R. L. Byer, "Quasi-phase-matched second harmonic generation: tuning and tolerances," IEEE J. Quantum Electron. **28**, 2631-2654 (1992).

15. M. E. Dearborn, K. Koch, G. T. Moore, and J. C. Diels, "Greater than 100% photon conversion efficiency from an optical parametric oscillator with intracavity difference-frequency mixing," in *Advanced Solid State Lasers*, paper PDP3, OSA Trends in Optics and Photonics 19 (Optical Society of America, Washington, DC), p. 240-244 (1998).

16. J. Fukumoto, H. Komine, J. W. H. Long, and J. R. K. Meyer, "Periodically poled $LiNbO_3$ optical parametric oscillator with intracavity difference frequency mixing on a single crystal," in *Conference on Lasers and Electro-Optics*, 1998 OSA Technical Digest Series 6 (Optical Society of America, Washington, DC), paper CPD5 (1998).

17. R. Wallenstein, "Laser sources for large frame projection displays," in *Center for Nonlinear Optical Materials Annual Affiliates Meeting*, (Stanford University, Stanford, CA) (1997).

18. U. Keller, *et al.*, "Semiconductor saturable absorber mirrors (SESAM's) for femtosecond to nanosecond pulsle generation in solid state lasers," IEEE J. Sel. Top. Quantum Electron. **2**, 435-453 (1996).

19. S. Tsuda, W. H. Knox, S. T. Cundiff, W. Y. Jan, and J. E. Cunningham, "Mode-locking ultrafast solid -state lasers with saturable Bragg reflectors," IEEE J. Sel. Top. Quantum Electron. **2**, 454-464 (1996).

20. W. Koechner. *Solid-State Laser Engineering* (Springer-Verlag, New York, 1996).

21. G. J. Spühler, *et al.*, "Diode-pumped passively modelocked Nd:YAG laser with 10-W average power in a diffraction-limited beam," Opt. Lett. **24**, 528-530 (1999).

22. A. Nebel, B. Ruffing, and R. Wallenstein, "A high-power diode-pumped all-solid-state RGB laser source," in *Conference on Lasers and Electro-Optics*, 1998 OSA Technical Digest Series 6 (Optical Society of America, Washington, D.C.), paper CPD3 (1998).

23. L. E. Myers, R. C. Eckardt, M. M. Fejer, R. L. Byer, W. R. Bosenberg, and J. W. Pierce, "Quasi-phasematched optical parametric oscillators in bulk periodically poled $LiNbO_3$," J. Opt. Soc. Am. B **12**, 2102-2116 (1995).

24. T. Graf, G. McConnell, A. Ferguson, E. Bente, D. Burns, and M. D. Dawson, "Synchronously pumped optical parametric oscillation in periodically poled lithium niobate with 1-W average output power," Appl. Opt. **38**, 3324-3328 (1999).

25. M. J. McCarthy and D. C. Hanna, "All-solid-state synchronously pumped optical parametric oscillator," J. Opt. Soc. Am. B **10**, 2180-2190 (1993).

26. G. D. Boyd and D. A. Kleinman, "Parametric interaction of focused Gaussian light beams," J. Appl. Phys. **39**, 3596-3639 (1968).

27. D. H. Jundt, "Temperature-dependent Sellmeier equation for the index of refraction, n_e, in congruent lithium niobate," Opt. Lett. **22**, 1553-1555 (1997).

28. D.-W. Chen and K. Masters, "CW 4.3 μm intracavity difference frequency generation in an optical parametric oscillator," in *Advanced Solid State Lasers*, TuA3, OSA Technical Digest (Optical Society of America, Washington, DC), p. 187-189 (2000).